Sensor and Simulation Notes

Note 459

High-Power Scanning Waveguide Array

Carl E. Baum

Air Force Research Laoratory
Directed Energy Directorate

Abstract

This paper considers the adaptation of scanning waveguide arrays to handle high power. By dividing a rectangular waveguide into subguides leading to subapertures one can avoid the use of small coupling holes in a waveguide. Then, using the dispersive character of the $H_{1,0}$ mode, the beam is radiated by the array in a desired direction. By varying the frequency of the source feeding the array the beam can be made to scan in the usual way.

This work was sponsored in part by the Air Force Office of Scientific Research, and in part by the Air Force Research Laboratory, Directed Energy Directorate.

1. Introduction

Microwave antennas for hypoband (narrow band) operation are a well-established subject. For high-power application, with electric fields approaching breakdown in various media of interest, the subject is less well established. However, some basic techniques for radiating high-power microwaves (HPM) have been published in several papers [1-3, 7]. These have been summarized in a book [16]. Among other things, these give techniques and canonical designs for HPM antenna systems (including waveguides) for pyramidal-horn fed reflector antennas for both high power and high gain. While these are quite appropriate HPM radiators, it is useful to consider other possible types for their potential advantages/disadvantages.

Array antennas, while more complex, have the advantage of having less depth (and hence less volume) for the same total antenna aperture, and hence similar potential antenna gain. A common form of an array is formed by a set of slots in one or more rectangular waveguides [11, 14]. (However, small holes are not appropriate for high power transmission through them.) Using the dispersive character of the lowest order waveguide mode ($H_{1,0}$) one can steer the antenna beam by changing the microwave frequency. Other types of guiding structures (e.g., dielectrics) have also been used for this purpose. However, for frequencies around a GHz the large size of the waveguides suggests that for low mass a hollow metal pipe has certain advantages.

In [1 (Section VI)] I have discussed the division of a rectangular waveguide into a set of subguides by insertion of metal sheets parallel to the broad wall (and perpendicular to the electric field of the $H_{1,0}$ mode) inside the waveguide and connecting to the side (narrow) walls. There, among other things, I suggested that this technique could be used to divide the power in the waveguide into N subguides which could be used to feed N array elements. The present paper expands on this in one form of such an array.

2. Division of Rectangular Waveguide into Subguide Feeding Subapertures

Begin with a rectangular waveguide a wide by b high as indicated in Fig. 2.1A. Let the cross-section dimensions be related in the usual way as

$$a = 2b \tag{2.1}$$

The details of the waveguide modes are discussed in various places [1, 15]. Our interest is in the lowest order mode, the $H_{1,0}$ (or $TE_{1,0}$) mode. The cutoff wavelength is

$$\lambda_c \equiv \lambda_{h,1,0} = 2a \tag{2.2}$$

with the traditional choice in (2.1) (for maximum power handling) the cutoff wavelength for the next H mode as well as the lowest E mode is a, exactly half that in (2.2). Operating with wavelength (in plane wave) between these two gives a 2:1 operating bandwidth without overmoding (a well-known microwave design principle).

There is only an E_y for the electric field proportional to $\sin(\pi x / a)$ in this lowest mode. The magnetic field has an x component (transverse) proportional to $\sin(\pi x / a)$ and a z component (longitudinal) proportional to $\cos(\pi x / a)$. As such we can introduce thin metal sheets (approximated as perfectly conducting) on planes of constant y, connecting to the side walls as illustrated in Fig. 2.1A without disturbing this $H_{1,0}$ mode. With $N-1$ such sheets uniformly spaced we have N subguides, each of width a and height b / N.

Having launched the mode into the subguides we can replace the conducting sheets by two initially touching sheets so that we can bend each subguide somewhat independently as discussed in [1]. Using typical microwave engineering practice we can route these guides to separate places to deliver N^{-1} of the microwave power to each such place (such as a radiating element of an array).

An example of a one-dimentional array is formed by extending the subguides to progressively different lengths as indicated in Fig. 2.1B. This produces a fan beam with a narrow beam in the z direction, but a broad beam in the $\pm x$ direction.

There are various ways to route the subguides to the subapertures. As shown in Fig. 2.2A, one way to do this does not require that the broad walls of adjacent subguides be separated. As one bends the subguides toward the $+y$ direction the local height $h(\zeta)$ (spacing between broadwalls) is allowed to expand smoothly. This lowers the electric field as one increases ζ with (as in Fig. 2.2B)

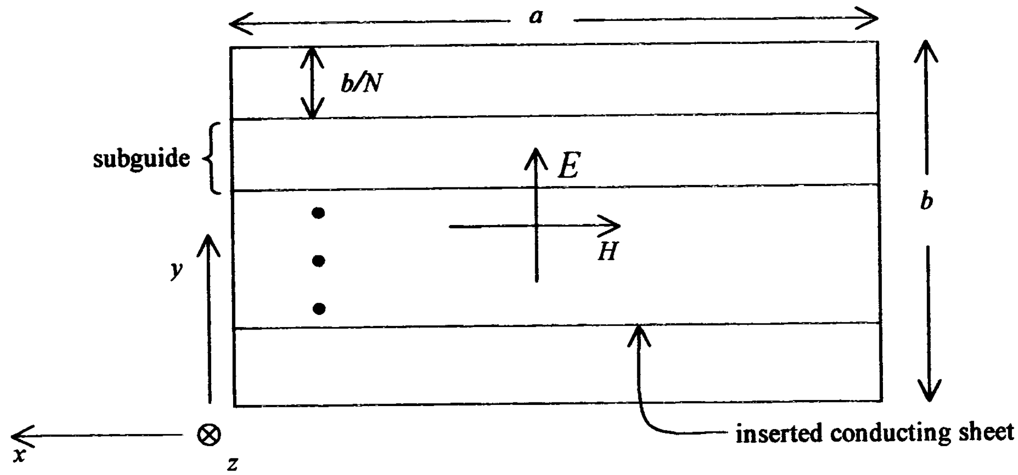

A. Cross-section view

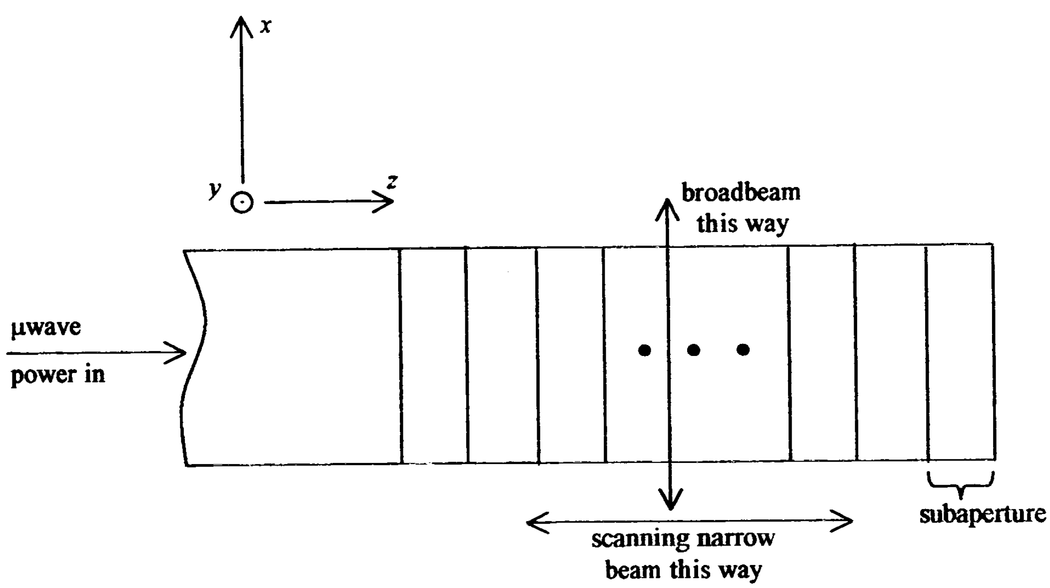

B. View perpendicular to broadwall (different scale)

Fig. 2.1 Subdivision of Rectangular Waveguide to Form Array

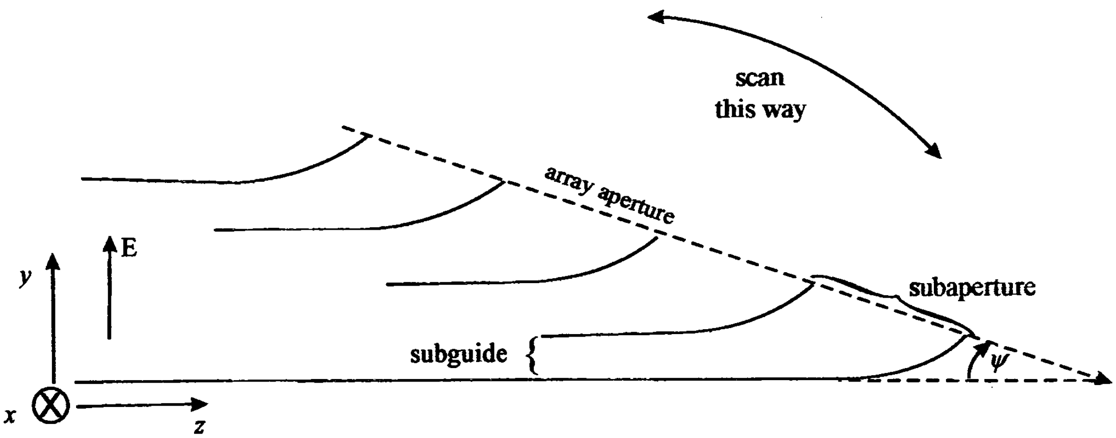

A. Side view

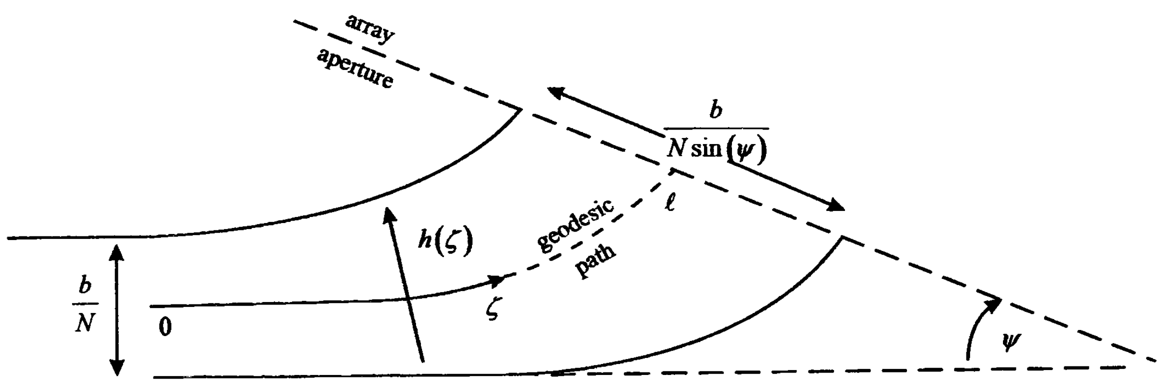

B. Single subguide

Fig. 2.2 Details of Transition of Subguides to Array

$$\begin{aligned} &0 \leq \zeta \leq \ell \\ &h(0) = \frac{b}{N} \\ &h(\ell) \leq \frac{b}{N \sin(\psi)} \end{aligned} \tag{2.3}$$

in going from the subguide entrance to the subaperture. Note the angle ψ which the aperture plane makes with a constant -y plane. This is somewhat under our control. Smaller ψ increases the aperture length and narrows the beamwidth in this direction.

At the subaperture one may wish to keep $h(\ell) \leq b$ to avoid overmoding there (if one wishes to operate at frequencies near the entry of the next propagating modes). If we choose the geodesic path for ζ to be perpendicular to the aperture plane on reaching it, this would give equality for $h(\ell)$ in (2.3) and place a constraint on ψ as

$$\sin(\psi) \leq N^{-1} \tag{2.4}$$

making small ψ require large N. However, the perpendicular geodesic path need not be enforced. Note that high electric fields in the waveguide may need to be reduced in going through the subguides to avoid breakdown in the air or other medium beyond the aperture plane. Some dielectric barrier may be on the aperture plane to separate the guide medium (e.g., vacuum) from the external medium.

The constraint on ψ in (2.4) can be relaxed by increasing the effective value of N by the technique illustrated in Fig. 2.3. After a subguide $h(\zeta)$ has increased to some value approaching b, it can be bifurcated (or divided by some larger number) so that $h(\zeta)$ is replaced by $h(\zeta)/2$ to continue increasing along a subsubguide toward a subsubaperture. This has effectively replaced N by $2N$ in (2.4). This procedure can be extended as far as one wishes.

Note that other paths might be taken by some of the guides (e.g., meandering as in [4]) to extend their lengths so that we have an ℓ_n for $n = 1, 2, \ldots, N$ so as better to adjust the phase along the aperture plane. Alternately one may introduce other media, or modify the walls (e.g., corrugation) to slow the wave speed in certain of the subguides.

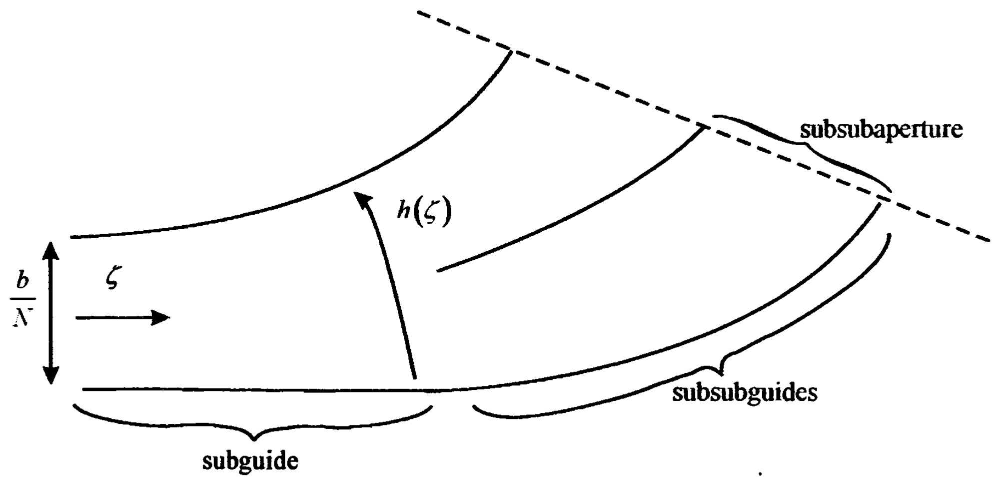

Fig. 2.3 Further Subdivision of Subguides

3. Scanning Properties

Assuming that the waveguide medium is characterized by permeability μ_0 and permittivity ε_0 (vacuum, gas) we have the free-space wavelength

$$\lambda = \frac{c}{f} = \frac{2\pi c}{\omega} \quad , \quad c = \left[\mu_0 \ \varepsilon_0\right]^{-1/2} \tag{3.1}$$

This and other formulae can be simply changed if some other uniform isotropic dielectric fills the waveguide. However, for our case a large λ for a given frequency f is desirable if our requirement is to have the array radiate into free space.

Then we define

$$\begin{aligned} f_1 &\equiv \frac{c}{\lambda_c} = \frac{c}{2a} \equiv \text{cutoff frequency for lowest mode} \\ f_2 &\equiv \frac{c}{2b} = \frac{c}{a} \equiv \text{frequency for next propagating mode to enter} \end{aligned} \tag{3.2}$$

Our operating range of frequencies is then

$$f_1 < f < f_2 = 2f_1 \tag{3.3}$$

Summarizing the well-known dispersion characteristics of the waveguide we have propagation in the waveguide in the form $e^{j\left[\omega t - k_g z\right]}$ with

$$\begin{aligned} k_g^2 &= k^2 - k_c^2 \quad , \quad \lambda_g^{-2} = \lambda^{-2} - \lambda_c^{-2} \\ k_c &= \frac{\omega_1}{c} = \frac{2\pi f_1}{c} = \frac{2\pi}{\lambda_c} \\ k &= \frac{\omega}{c} = \frac{2\pi f}{c} \\ \frac{\lambda}{\lambda_g} &= \frac{k_g}{k} = \left[1 - \left[\frac{\lambda}{\lambda_c}\right]^2\right]^{\frac{1}{2}} = \left[1 - \left[\frac{f_1}{f}\right]^2\right]^{\frac{1}{2}} \end{aligned} \tag{3.4}$$

Note that as $f \to f_1$ the guide wavelength $\lambda_g \to \infty$, an important property for feeding the array.

Let all the subguides as in Fig. 2.2 be identical (translation symmetry) with length ℓ, height $h(\zeta)$, and width a. Then the phase shifts (or delays) in all subguides are the same. The problem then reduces to that in Fig. 3.1 with the guide propagation in the z direction matching to the array beam direction as

$$k_g \cos(\psi_1) = k \cos(\psi_2) \tag{3.5}$$

(also known as Snell's law) with ψ_1 identified as ψ. We can regard ψ_2 (or $\pi/2 - \psi_2$) as the array scan angle.

Solving for ψ_2 we have

$$\psi_2 = \arccos\left(\frac{k_g}{k}\cos(\psi_1)\right) = \arccos\left(\frac{\lambda}{\lambda_g}\cos(\psi_1)\right) \tag{3.6}$$

Noting that in the operating range of interest

$$0 < k_g < k \quad , \quad \infty > \lambda_g > \lambda \tag{3.7}$$

we then have

$$\psi_1 < \psi_2 < \frac{\pi}{2} \tag{3.8}$$

Note that the bend direction is away from the array surface due to the waveguide dispersion characteristic which makes $\lambda_g > \lambda$. This is opposite in sense to a wave coming out of a dielectric medium into free space [5]. With the restriction on f in (3.3) for no overmoding we have

$$0 < \frac{\lambda}{\lambda_g} = \frac{k_g}{k} < \left[\frac{3}{4}\right]^{\frac{1}{2}} \simeq 0.866 \tag{3.9}$$

This gives a tighter restriction on ψ_2 as

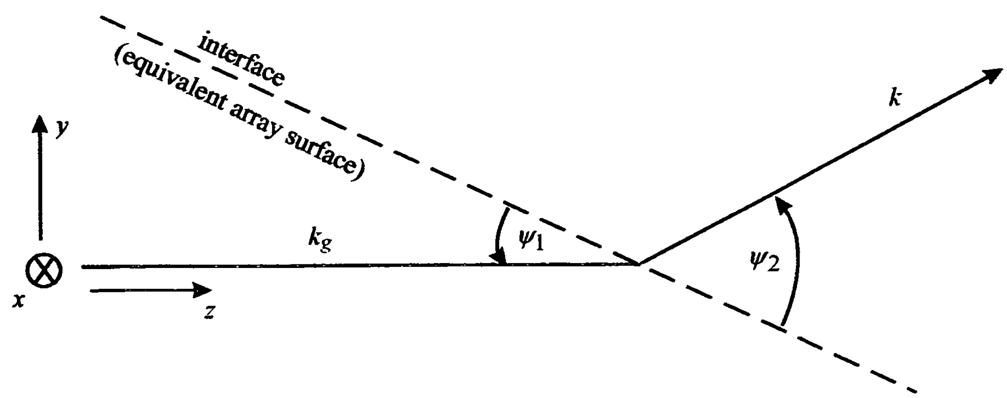

Fig. 3.1 Array Scan Angle

$$\arccos\left(\left[\frac{3}{4}\right]^{\frac{1}{2}}\cos(\psi_1)\right) < \psi_2 < \frac{\pi}{2} \tag{3.10}$$

for f near f_1 (k_g near zero) we have the asymptotic forms

$$\begin{aligned}
\arccos\left(\frac{k_g}{k}\cos(\psi_1)\right) &= \frac{\pi}{2} - \arcsin\left(\frac{k_g}{k}\cos(\psi_1)\right) \\
&= \frac{\pi}{2} - \frac{k_g}{k}\cos(\psi_1) + O\left(\left[\frac{k_g}{k}\right]^3\right) \\
&\qquad \text{as } \frac{k_g}{k} = \frac{\lambda}{\lambda_g} \to 0 \\
\frac{k_g}{k} = \frac{\lambda}{\lambda_g} &= \left[1-\left[\frac{f_1}{f}\right]^2\right]^{\frac{1}{2}} = \frac{f_1}{f}\left[\left[\frac{f}{f_1}+1\right]\left[\frac{f}{f_1}-1\right]\right]^{\frac{1}{2}} \\
&= 2^{1/2}\left[\frac{f}{f_1}-1\right]^{\frac{1}{2}}\left[1+O\left(\frac{f}{f_1}-1\right)\right] \\
&\qquad \text{as } \frac{f}{f_1} - 1 \to 0
\end{aligned} \tag{3.11}$$

With these results one can see what range of ψ_2 (scan angle) can be achieved for a given range of f. This range of f is determined by the range of frequencies over which the source can be tuned. At high power levels such tuning can be difficult depending on how fast (scan rate) one wishes to change the frequency to correspond to some range of scan angle.

4. Tapered Subguides

Now consider some properties of the taper of the subguides as in Fig. 2.2B. The $H_{1,0}$ mode has transverse fields E_y and H_x varying across the guide as $\sin(\pi\, x / a)$ with a modal impedance

$$\frac{E_y}{H_x} = Z_h = \frac{k}{k_g} Z_0 \quad , \quad Z_0 = \left[\frac{\mu_0}{\varepsilon_0}\right]^{1/2} \tag{4.1}$$

Keeping the width a constant then Z_h does not change, even as the height is varied.

In the taper we have the same propagating mode as long as we restrict $h(\zeta) < b$ (or a little larger if we are not operating close to the cutoff frequency of the next mode). Let us then let $h(\zeta)$ vary in a monotonically increasing fashion for $0 \le \zeta \le \ell$ as in (2.3). Furthermore, let the relative change in $h(\zeta)$ be small over a wavelength, i.e., let

$$\frac{\lambda_g}{h(\zeta)} \frac{dh(\zeta)}{d\zeta} = \lambda_g \frac{d\ell n(h(\zeta))}{d\zeta} << 1 \tag{4.2}$$

Under this approximation the reflections of the mode in the subguide are small. We can then estimate the fields reaching $\zeta = \ell$ by conserving power, giving

$$\frac{|E\|_{\zeta=\ell}}{|E_y\|_{\zeta=0}} = \left[\frac{h(\ell)}{h(0)}\right]^{1/2} \tag{4.3}$$

Of course, there will in general be some reflections back to $\zeta = 0$. These can be estimated by more detailed calculations [6, 9, 13].

There are various ways to smoothly taper $h(\zeta)$. A simple one is the exponential taper given by [8]

$$\frac{h(\zeta)}{h(0)} = e^{\frac{\zeta}{\zeta_0}} \quad , \quad \zeta_0^{-1} = \frac{1}{\ell} \ell n\left(\frac{h(\ell)}{h(0)}\right) \tag{4.4}$$

There are other commonly used tapers for broadband performance, such as the Chebyshev taper [12].

At $\zeta = \ell$ the subguide feeds a subaperture. This can introduce undesirable reflections back into the subguide. Various tuning devices can be placed in each subguide near $\zeta = \ell$ to reduce these reflections [10]. Note that the waves emitted from adjacent subapertures can also couple back into the subaperture; allowance needs to be made for this.

5. Subguide Exits into Subapertures

In going through the subaperture one may transition from one dielectric medium such as vacuum to another such as air. Figure 5.1 shows a way to accomplish this based on the technique discussed in [1]. A thin dielectric diaphragm can be supported against the pressure differential by the use of metal slats perpendicular to the electric field, thereby not interfering with the transmission of the wave through the subaperture. The slats connect to both side walls of the subguide for mechanical support. Further details are discussed in [1].

We can have a flat interface as in Fig. 5.1A, or the dielectric sheet can be bent as in Fig. 5.1B to increase the tracking distance and theregy reduce the electrical-breakdown problem. While the slats are on the inside (in the subguides) in the illustration to hold out the exterior gas, the slats could be placed outside if the subguides were pressurized (e.g., with SF_6).

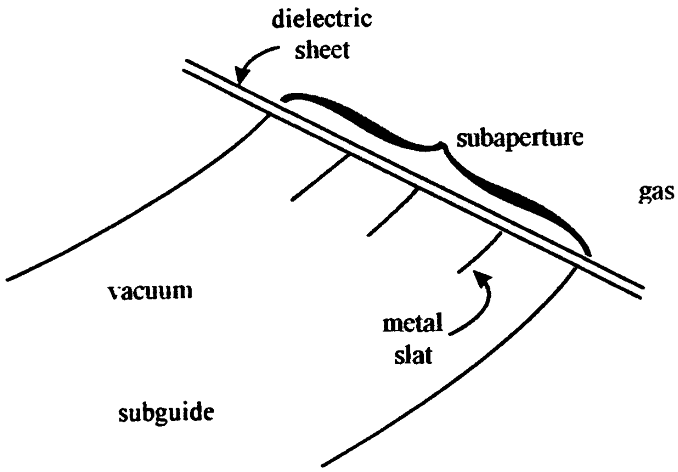

A. Flat dielectric sheet

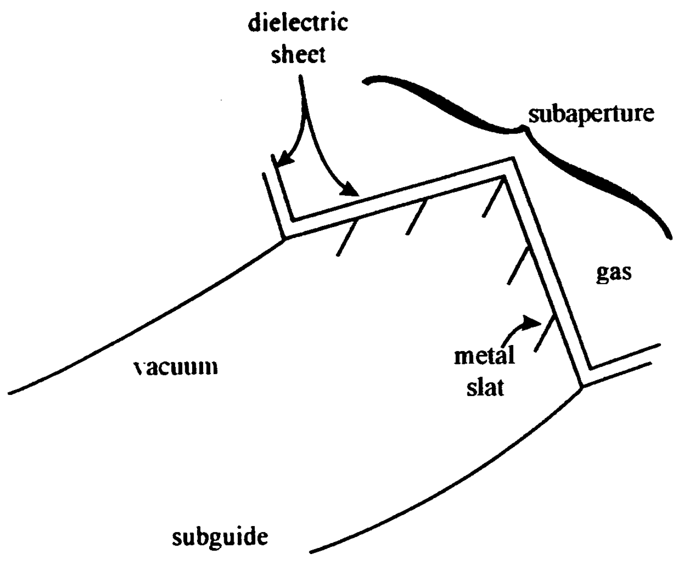

B. Sloped dielectric sheets

Fig. 5.1 Vacuum/Gas Interface at Subaperture

6. Multiple Divided Rectangular Waveguides

The basic waveguide array shown in Figs. 2.1 and 2.2 can be extended to two or more such subdivided waveguides to form a larger array such as illustrated in Fig. 6.1. With the parallel arrangement shown there the fan beam can be narrowed in the $\pm x$ direction. The phase of the waves in the two guides must be controlled in a relative sense. This can be accomplished by a power splitter from a single microwave source.

This power splitter can include some differential phase shift between the two waveguides to orient the beam center in the $\pm x$ direction, if desired. However, it may be difficult to rapidly change this phase shift (using mechanical motion of dielectrics, etc.). This is in contrast to the "electronic" scanning in the $\pm z$ direction by variation of the source frequency.

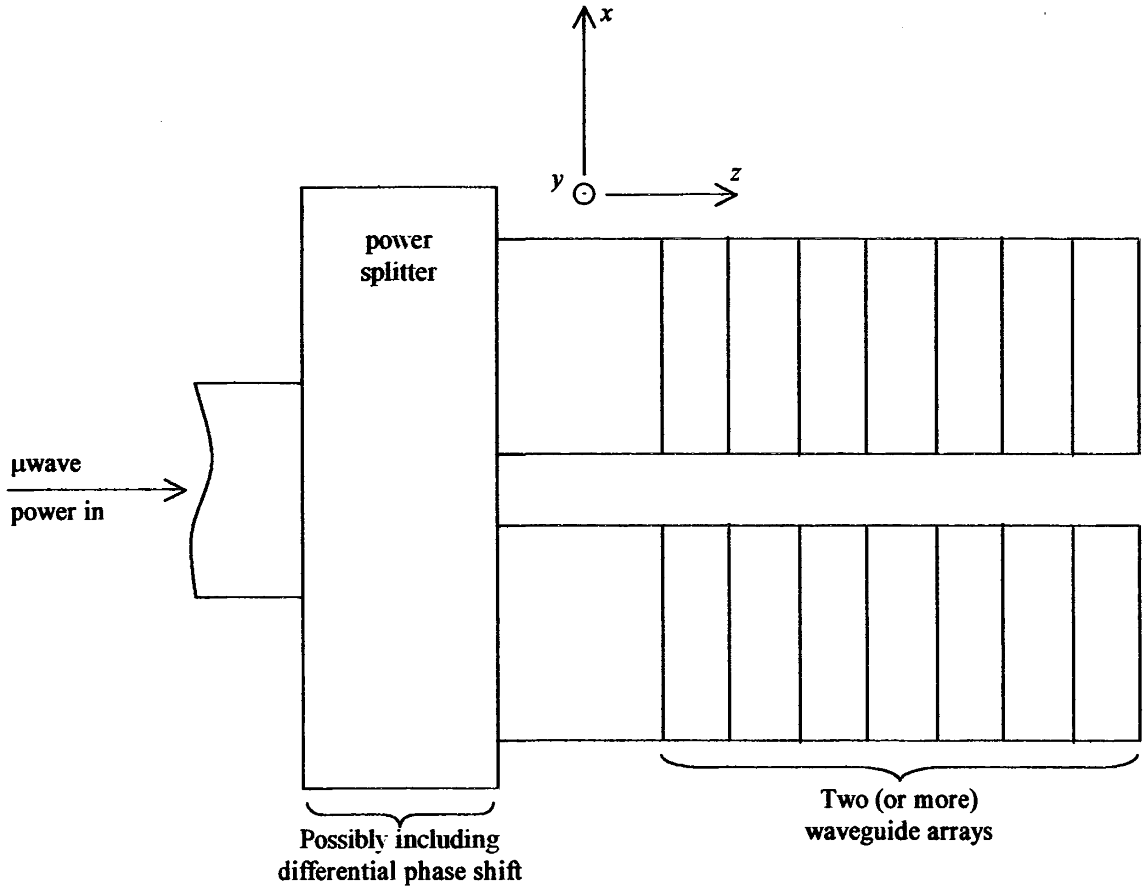

Fig. 6.1 Extension to Multiple-Waveguide Arrays

7. Concluding Remarks

So here we have a scanning waveguide array based on traditional principles, but extended into the high-power regime. When operated at a single frequency such an array merely compresses the antenna depth toward an aperture plane as compared to a standard horn-fed paraboloidal reflector. However, the array is a more complex structure. When operated with a frequency-agile source this array becomes an antenna with a beam which scans in one coordinate. The scanning rate depends on how fast the frequency can be shifted.

While this paper outlines the basic features of a high-power scanning waveguide array, there are many details to be considered. This entaisl both calculations and experimental optimizations.

References

1. C. E. Baum, "Some Features of Waveguide/Horn Design", Sensor and Simulation Note 314, November 1988.

2. D. V. Giri, "Canonical Examples of High-Power Microwave (HPM) Radiation Systems for the Case of One Feeding Waveguide", Sensor and Simulation Note 326, April 1991.

3. Y. Rahmat-Samii, D. W. Duan, and D. V. Giri, "Canonical Examples of Reflector Antennas for High Power Microwave Applications", Sensor and Simulation Note 334, October 1991.

4. C. E. Baum, "Arrays of Parallel Conducting Sheets for Two-Dimensional E-Plane Bending Lenses", Sensor and Simulation Note 341, April 1992.

5. C. E. Baum, "Steerable Lens Surface for Use with the IRA Class of Antennas", Sensor and Simulation Note 387, September 1995.

6. C. E. Baum, "Matching Modulated Electron Beam to Waveguide", Circuit and Electromagnetic System Design Note 39, April 1990.

7. D. V. Giri, "Preliminary Considerations for High-Power Microwave (HPM) Radiating System", Circuit and Electromagnetic System Design Note 40, December 1990.

8. C. E. Baum, "Nonuniform Transmission-Line Transformers for Fast High-Voltage Transients", Circuit and Electromagnetic System Design Note 4, February 2000.

9. L. Solymar, "Spurious Mode Generation in Nonuniform Waveguide", IRE Trans. Microwave Theory and Techniques, 1959, pp. 379-383.

10. C. G. Montgomery, R. H. Dicke, and E. M. Purcell, *Principles of Microwave Circuits*, McGraw-Hill, 1948.

11. M. J. Ehrlich, "Slot-Antenna Arrays", ch. 9, in H. Jasik (ed.), *Antenna Engineering Handbook*, McGraw-Hill, 1961.

12. R. E. Collin, *Foundations for Microwave Engineering*, McGraw-Hill, 1966.

13. L. Lewin, *Theory of Waveguides*, Wiley, 1975.

14. R. Tang, "Practical Aspects of Phased Array Design", ch. 18, in Y. T. Lo and S. W. Lee (eds.), *Antenna Handbook*, Van Nostrand Reinhold, 1988.

15. R. E. Collin, *Field Theory of Guided Waves*, IEEE Press, Oxford U. Press, 1991.

16. C. D. Taylor and D. V. Giri, *High-Power Microwave Systems and Effects*, Taylor & Francis, 1994.